International Journal of Pharmaceutics 398 (2010) 73–82

Contents lists available at ScienceDirect

International Journal of Pharmaceutics

journal homepage: www.elsevier.com/locate/ijpharm

Computational oral absorption simulation of free base drugs

Kiyohiko Sugano*

Global Research & Development, Sandwich Laboratories, Research Formulation, Pfizer Inc., CT13 9NJ Sandwich, Kent, UK

ARTICLE INFO

Article history:
Received 20 May 2010
Received in revised form 15 July 2010
Accepted 17 July 2010
Available online 23 July 2010

Keywords:
Free base
Solubility
Dissolution rate
Computational simulation
Oral absorption

ABSTRACT

The purpose of the present study was to investigate the oral absorption simulation of free base drugs. In the case of a low solubility free base drug, a portion of drug particles remains incompletely dissolved during the stomach transit and can reach the small intestine. As the pH is neutralized in the small intestine, the solubility of the drug decreases and the concentration gradient around the particles becomes a negative value. The drug particles would then grow because of this negative concentration gradient resulting in a reduction of the dissolved drug concentration. The modified Nernst Brunner equation was used to simulate both particle dissolution and growth (particle growth is the opposite phenomena of particle dissolution). Albendazole, aprepitant, dipyridamole, gefitinib and ketoconazole were used as model drugs (all free solid form (not salts)). The effect of stomach pH on oral absorption was appropriately simulated. Based on the simulation results, it was suggested that the dissolution patterns in the gastrointestinal tract were significantly different depending on the dose–solubility ratio in the stomach.

1. Introduction

Computational oral absorption simulation (COAS) is anticipated to be a useful tool in drug discovery and development (van de Waterbeemd and Gifford, 2003). To enable a mechanistic approach, the theoretical equations of dissolution, precipitation (nucleation), permeation and gastrointestinal transit were compiled as a gastrointestinal unified theoretical framework (GUT framework) (Sugano, 2009b), in which various drug molecular states (free undissociated monomer, bile micelle bound molecule, etc.), drug molecular properties (dissociation constant, solubility, bile partition coefficient, surface activity, etc.), drug substance properties (particle size, particle shape, free/salt form (including solubility product), etc.), drug product properties (immediate release, controlled release, etc.), permeation pathways (unstirred water layer, passive transcellular, etc.), physiological conditions (pH, bile micelles, buffer capacity, agitation strength, etc.) and morphological parameters (fold and villi structure, etc.) are explicitly taken into account. Previously, the GUT framework has been applied and validated for the cases when the stomach has little effect on oral absorption, i.e., the oral absorption of low solubility undissociable and free acidic drugs, and high solubility–low permeability drugs. The GUT framework was found to appropriately simulate the fraction of a dose absorbed (*Fa*) (Sugano, 2009a,c), species differences (Sugano, 2009f), particle size dependency (including nano-particles) (Sugano, 2009f, 2010), dose dependency and the food effects (Sugano et al., 2010). Therefore, in the cases where the stomach has little effect on oral absorption, the GUT framework was validated by various in vivo data. However, a low pH in the stomach adds another dimension of difficulty in COAS.

Since pH in the stomach is lower than that in the small intestine, a basic compound shows higher solubility in the stomach than in the small intestine. Therefore, in the case of a basic drug which has a low solubility in the small intestinal fluid, the drug molecule once dissolved in the stomach can precipitate out in the small intestine. The precipitation process can be divided into two steps, nucleation and particle growth (the latter is the reverse process of dissolution). The active pharmaceutical ingredient (API) of a basic drug can be categorized into two types, free base and salts. The difference of these two solid forms in the GUT framework is that, for a salt form, a nucleation model equation is required to simulate the precipitation of a new free form after dissolution of the salt, whereas it would not be required for a free form API since a portion of the free form solid particles are not completely dissolved during the passage through the stomach and reach the small intestine as undissolved solid particles which become nuclei particles for precipitation (Johnson, 2003; Sugano, 2009b). In this article, the oral absorption of free base drugs is focused.

In the GUT framework, the Nernst Brunner (NB) equation was modified to take the difference between the bulk fluid and solid surface pHs into account (Sugano et al., 2007). This modified NB (mNB) equation can be used to calculate both the dissolution and "particle growth" of API. The API particles dissolve or grow depending on the concentration gradient (ΔC) of dissolved drug molecule around a particle, i.e., ΔC being positive for dissolution and negative for particle growth. Since the pH in the stomach is lower than that

* Tel.: +44 1304 644338.
E-mail address: Kiyohiko.Sugano@pfizer.com.

0378-5173/$ – see front matter © 2010 Elsevier B.V. All rights reserved.
doi:10.1016/j.ijpharm.2010.07.027

of the small intestine, as the stomach fluid (which contains both dissolved drug molecules and undissolved drug particles) pours into the small intestine, the pH was neutralized, and the dissolved drug concentration ($C_{dissolv}$) in the small intestine becomes higher than the equilibrium (saturated) solubility of a drug at a neutral pH, resulting in a negative ΔC and particle growth in the small intestine.

Even though the mechanistic theoretical framework has been proposed to simulate the oral absorption of free base drugs in the GUT framework, a verification study has not been reported. The purpose of the present study was to apply the GUT framework for oral absorption simulation of free base drugs and demonstrate that the mNB equation can be used to simulate the concentration reduction by the particle growth in the small intestine. Albendazole, aprepitant, dipyridamole, gefitinib and ketoconazole were used as model drugs, since a full set of physicochemical data and clinical oral absorption data are available in the literature.

2. Method

The GUT framework was previously reported in detail (Okazaki et al., 2008; Sugano, 2008, 2009a,b,c,e, 2010), therefore, only briefly explained in the following sections. In the GUT framework, the dissolved amount of a drug is defined as the sum of unbound monomer and bile micelle bound molecules for the standard formulation cases.

2.1. Modified Nernst Brunner equation

The mNB equation was used to represent both dissolution and particle growth in the gastrointestinal (GI) tract. In the modified mNB equation, the solid surface solubility ($S_{surface}$) was taken into account.

$$\sum_{ij} \frac{dX_{undissolv,ij}}{dt} = -\frac{dX_{dissolv}}{dt} = \sum_{ij} -\frac{3 \cdot D_{eff}}{r h_p \rho} X_{undissolv,ini,ij}^{1/3} \cdot X_{undissolv,ij}^{2/3} \cdot \Delta C \quad (1)$$

$$\Delta C = S_{surface}\left(1 - \frac{X_{dissolv}}{V_{GI} S_{dissolv}}\right) = S_{surface}\left(1 - \frac{C_{dissolv}}{S_{dissolv}}\right) \quad (2)$$

where $X_{undissolv}$ and $X_{dissolv}$ are the undissolved and dissolved drug amount (weight or molar), respectively, D_{eff} is the effective diffusion coefficient in bile micelle media, r is the particle radius, ρ is the true density of the drug particles estimated from the chemical formula (Cao et al., 2008), h_p is the effective thickness of the unstirred water layer on the drug particles, $S_{dissolv}$ is the solubility of a drug in bile micelle media such as the fasted state simulated intestinal fluid (FaSSIF) (Galia et al., 1998), $S_{surface}$ is the solubility at the solid surface, and V_{GI} is the volume of the gastrointestinal fluid. The subscripts i and j represent the particle size and virtual particle size bins, respectively. At the beginning of dissolution, $C_{dissolv} \ll S_{dissolv}$, therefore $\Delta C \approx S_{surface}$. Eq. (1) is a first approximation to appropriately treat the dissolution rate and saturated solubility simultaneously in an equation.

The effective diffusion coefficient in a bile micelle media was calculated as:

$$D_{eff} = D_{mono} \cdot f_{mono} + D_{bm} \cdot f_{bm} \quad (3)$$

where D_{mono} and D_{bm} are the diffusion coefficients of free monomer and bile micelle bound molecules, respectively, and f_{mono} is the fractions of free monomer. D_{mono} was estimated as $D_{mono} = 9.9 \times 10^{-5}\ MW^{-0.453}$ (Avdeef, 2010). D_{bm} in the fasted state simulated intestinal fluid (FaSSIF) was set to $0.12 \times 10^{-6}\ cm^2/s$ (Okazaki et al., 2008). f_{mono} was calculated as $S_{blank}/S_{dissolv}$ where S_{blank} is the solubility in the blank buffer without bile micelles.

h_p was calculated by the fluid dynamic model as previously reported (Sugano, 2008). The agitation strength in the GI tract was assumed to be equivalent to that of the USP paddle method with 50 rpm. When the terminal velocity of a particle was less than 0.0023 m/s, it was assumed that the particle sediments on the wall of the intestine and the asymptotic diffusion occurred as the dissolution process (i.e., $h_p = r_p$).

2.2. P_{eff} estimation

The permeation rate constant (k_{perm}) and the effective intestinal membrane permeability coefficient (P_{eff}) were estimated as previously reported.

$$\frac{dX_{abs}}{dt} = k_{perm} \cdot C_{dissolv} \cdot V_{GI} = \frac{2}{R_{GI}} \cdot DF \cdot P_{eff} \cdot C_{dissolv} \cdot V_{GI} \quad (4)$$

$$P_{eff} = \frac{1}{(1/(D_{eff}/h_{UWL}) + P_{WC}) + (1/(f_{mono} \cdot (f_0 \cdot P_{trans,0} + P_{para}) \cdot Acc \cdot VE))} \cdot PE \quad (5)$$

where X_{abs} is the amount of the drug absorbed into the body, DF is the degree of flatness of the intestinal tube, R_{GI} is the radius of the intestine, h_{UWL} is the thickness of the unstirred water layer (UWL) on the intestinal membrane, P_{WC} is the UWL permeability by water conveyance, Acc is the accessibility of a drug to the epithelial membrane (Oliver et al., 1998), VE is the surface expansion ratio by the villi structure, and PE is the surface expansion ratio by the plicate structure. According to the pH partition theory, passive transcellular permeation was estimated by the undissociated fraction (f_0) and intrinsic transcellular permeability ($P_{trans,0}$). P_{para} is the paracellular permeability coefficient calculated based on the negatively charged sieve permeation model using the pore radius and charge for humans (Adson et al., 1994; Sugano et al., 2002, 2003; Sugano, 2009f). $P_{trans,0}$ is calculated from the octanol/water partition coefficient (P_{oct}) as (Avdeef et al., 2005; Sugano, 2009a),

$$P_{trans,0}\ (cm/s) = 2.36 \times 10^{-6} {P_{oct}}^{1.1} \quad (6)$$

The model compounds used in this article are highly lipophilic. In this case, the rate-limiting step becomes the UWL permeability (first term in the dominator of Eq. (5)), rather than the epithelial membrane permeability. D_{bm} in the UWL was set to be threefold larger for FaSSIF (Li et al., 1996). For albendazole and aprepitant, a reduction in h_{UWL} by the particle drifting effect (PDE) was considered for P_{eff} calculation since the particle size is small and dose strength is high (Sugano, 2010). It was suggested that when the dose (mg)/particle diameter (μm) ratio exceeds 20, the particle drifting effect would become significant.

2.3. GI transit model and integration

The 1 stomach–7 small intestine–1 colon compartment system was used in this article (Sawamoto et al., 1997; Yu and Amidon, 1999). Drug particles and dissolved drug molecules were assumed to transfer between the compartments following the first order kinetics ($T_{1/2}$ = 10 min for the stomach and 21 min for each intestinal compartment) (Kortejaervi et al., 2007; Parrott et al., 2009). The dose volume was set to 225 mL and added to the stomach compartment with the settling volume of 25 mL (Dressman et al., 1998). The excretion of the stomach fluid (containing both undissolved and dissolved drug) into the first compartment of the small intestine was simulated to follow the first order kinetics with the settling volume of 25 mL (the secretion rate of the stomach fluid was set to 1.7 mL/min). The fluid volume in the small intestine was kept at 250 mL (36 mL for each compartment). The differential equations for dissolution, particle growth, permeation and

GI transit were simultaneously numerically integrated using 4th Runge–Kutta method with an integration step of 0.1 min for 8 h.

The particle size distribution was represented by assigning a bin to each particle size range. Twenty bins were used to represent the particle size distribution (i = 20, log-normal distribution with 0.3 log unit standard deviation). A particle size bin was further divided into 100 virtual bins (j = 100, except for albendazole) to represent the movement of particles in the GI tract (for albendazole, j = 500 was used to increase the accuracy in the single digit percent range of the fraction of a dose absorbed (*Fa%*)). Each virtual bin was triggered to start dissolving once the API particle is released from the formulation.

2.4. Drug and physiological parameters

The drug parameters of the model drugs are obtained from the literature and summarized in Table 1 (Diaz et al., 1998; Avdeef, 2003; Glomme et al., 2006; Takano et al., 2006, 2008; Vertzoni et al., 2007; Escher et al., 2008; Vogt et al., 2008; Parrott et al., 2009; Wilson et al., 2009). In the case of acid and base drugs, it is well known that the solid surface pH is affected by the dissolving drugs. In this study, according to Serajuddin et al. (Serajuddin, 2007; Pudipeddi et al., 2008), the experimental $S_{surface}$ values were taken from the literature (Table 1). In addition, the Mooney–Stella method was used to estimate the solid surface pH (Mooney et al., 1981). The modified Henderson–Hasselbalch equation was used to calculate the solubility from the pH, pK_a, bile micelle partition coefficient, bile micelle concentration and intrinsic solubility (Sugano, 2009b). Since particle size data of dipyridamole, gefitinib and ketoconazole were not available in the literature, they were estimated from the dissolution test data (Fig. 1) (Zhou et al., 2005). Previously, estimation of the particle size from the dissolution test data was shown to be appropriate (Avdeef et al., 2009). In addition, there are many reports showing that the mNB appropriately predicted the dissolution profile from the particle size data, suggesting that the mNB can be used to calculate the particle size from the dissolution data (Hintz and Johnson, 1989; Jinno et al., 2006; Okazaki et al., 2008).

Table 2
Physiological parameters for fasted humans[a].

	Position	Value
Morphology		
R_{GI}	Small intestine	1.5 cm
DF	Small intestine	1.7
PE	Small intestine	3
VE	Small intestine	10
GI transit		
T1/2	Stomach	10 min
	Small intestine	21 min[b]
Fluid property		
V_{GI}	Stomach	25 mL
	Small intestine	250 mL[c]
pH	Stomach	1.8/6.5
	Small intestine	6.5
Agitation strength	Stomach	50 rpm equiv.[d]
	Small intestine	50 rpm equiv.
Others		
h_{UWL}	Small intestine	300 μm
P_{WC}	Small intestine	0.23×10^{-4} cm/s

[a] Sugano (2009) and references there in.
[b] Mean small intestinal transit time = 3.5 h.
[c] 36 mL per each compartment.
[d] Agitation strength equivalent to 50 rpm in the USP paddle method.

The physiological parameters are summarized in Table 2. Clinically observed *Fa%* data were obtained from the clinical pharmacokinetic data, as discussed in detail in the following section.

3. Results and discussion

The simulated *Fa%*-time profiles and dissolved%-time profiles are shown in Fig. 2. The simulated concentration time profile in the

Table 1
Compound parameters[a].

	Albendazole	Aprepitant	Dipyridamole	Gefitinib	Ketoconazole
Phys. chem. properties					
MW	265.3	534.4	504.6	446.9	531.4
log P_{oct}	3.1	4.8	3.9	4.1	4.3
pK_a	4.2	4.2[j]	6.2	5.28, 7.17	2.9, 6.5
Density (g/cm^3)[b]	1.3	1.5	1.2	1.3	1.3
Intrinsic parameters					
Intrinsic solubility (mg/mL)	0.00055	0.0008	0.004	0.0007	0.006
D_{mono} ($\times 10^{-6}$ cm^2/s)[c]	7.9	5.8	5.9	6.2	5.8
$P_{trans,0}$ (cm/s)[d]	0.0061	0.45	0.046	0.076	0.13
Feeding parameters					
$S_{dissolve}$ (st[e]) (mg/mL)[f]	0.14[i]	0.20[i]	>30	>5.0	>30
$S_{surface}$ (st) (mg/mL)	0.14[i] (pH 1.8)	0.20[i] (pH 1.8)	8.6 (pH 3.1)	5.0 (pH 5.0)	9.0 (pH 3.5)
$S_{dissolve}$ (si[e]) (mg/mL)[g]	0.0021	0.006	0.017	0.085	0.021
S_{blank} (si) (mg/mL)[h]	0.00055	0.0008	0.006	0.0041	0.012
$S_{surface}$ (si) (mg/mL)	0.0021	0.006	0.017	0.085	0.021
D_{eff} (st) ($\times 10^{-6}$ cm^2/s)	7.9	5.8	5.9	6.2	5.8
D_{eff} (si) ($\times 10^{-6}$ cm^2/s)	2.2	0.87	2.2	0.42	3.3
P_{eff} (si) ($\times 10^{-4}$ cm/s) without PDE	2.9	1.8	3.0	1.2	4.1
P_{eff} (si) ($\times 10^{-4}$ cm/s) with PDE	6.5	8.5 (0.2 μm[k])	–	–	–

[a] Solubility, pK_a, and log P_{oct} data were taken from the literatures (Diaz et al., 1998; Avdeef, 2003; Glomme et al., 2006; Takano et al., 2006, 2008; Vertzoni et al., 2007; Escher et al., 2008; Vogt et al., 2008; Parrott et al., 2009; Wilson et al., 2009, aprepitant interview form; gefinitib interview form).
[b] Calculated from chemical formula (Cao et al., 2008).
[c] Calculated from MW (Avdeef, 2010).
[d] Calculated from P_{oct}.
[e] st = stomach, si = small intestine.
[f] Solubility in the blank buffer at pH 1.8.
[g] Solubility in the fasted state simulated intestinal fluid (FaSSIF) composed of 3 mM taurocholic acid and 0.75 mM phosphatidylcholine (pH 6.5).
[h] Solubility in the blank buffer at pH 6.5.
[i] pH and solubility were calculated by the Mooney–Stella and Henderson–Hasselbalch equations.
[j] Average value calculated by ACD V8.14 (pK_a = 4.02) and Pallas V3.0 (pK_a = 4.38).
[k] Particle size.

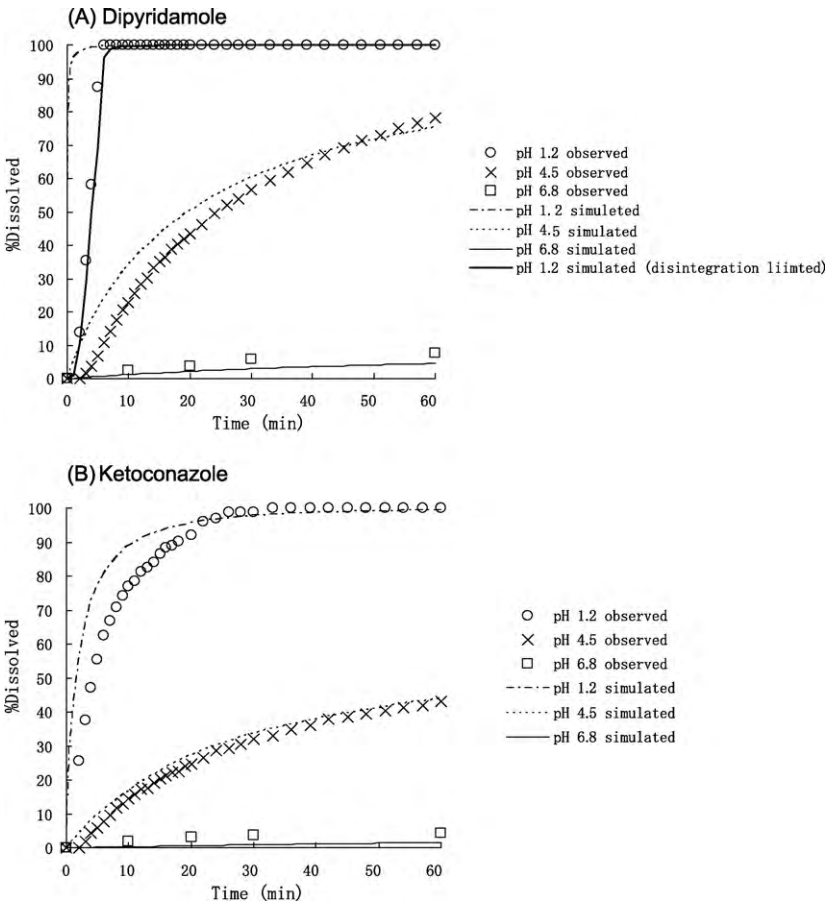

Fig. 1. Observed and simulated dissolution profiles in the USP paddle method. (A) Dipyridamole and (B) ketoconazole. The observed profiles were obtained from Zhou et al. (2005).

GI tract is shown in Fig. 3. The number of particles which remained incompletely dissolved during the stomach transition is shown in Fig. 4. Overall relationship between simulated and observed *Fa%* is summarized in Table 3 and shown in Fig. 5.

A qualitative correlation was observed between simulated and observed *Fa%* for free base drugs with various physicochemical properties and dose range (Table 3 and Fig. 4), suggesting that dissolution and particle growth in the GI tract could be simulated using the mNB equation for a rough estimation of *Fa%* in drug discovery and early drug development. The effect of the stomach pH on the oral absorption of weak base free drugs was appropriately captured by the simulation. This is important for developing an appropriate API form and formulation to mitigate the risk of the drug–drug interaction with antacids via stomach pH and variation of the exposure for hypoacid stomach patients (Morihara et al., 2001). However, the prediction accuracy was considered to be insufficient for late development (i.e., <10–20% error). The current approach tended to underestimate the *Fa%*, probably due to an underestimation of the real solubility of the drugs in the intestinal fluid (Clarysse et al., 2009), resulting in a non-linear relationship between predicted and observed *Fa%*. To improve the predictability, further improvements in the accuracy of drug and physiological parameters would be required (Lennernäs, 2007), as well as more sophisticated model equations.

Table 3
Clinical and simulated *Fa%*.

Drug name	Stomach pH	Dose (mg)[b]	Dose number		Particle size (μm)	*Fa%*	
			Stomach	Intestine		Observed	Simulated
Albendazole	Normal	1400	40	2667	10	3.8	1.1[d]
	High pH[a]	1400	–		10	2.7	1.1[d]
Aprepitant	Normal	100	2	67	5	19	8.6
	Normal	125			0.2	62	28[d]
Dipyridamole	Normal	50	<0.007	12	75[c]	57	59
	High pH[a]	50	–		75[c]	36	14
Gefitinib	Normal	250	<0.2	12	30[c]	73	76
	High pH[a]	250	–		30[c]	39	20
Ketoconazole	Normal	200	<0.03	38	200[c]	69	59
	High pH[a]	200	–		200[c]	5.8	5.1

[a] H2 blocker treated.
[b] See text.
[c] Calculated from the dissolution test.
[d] PDE was taken into account.

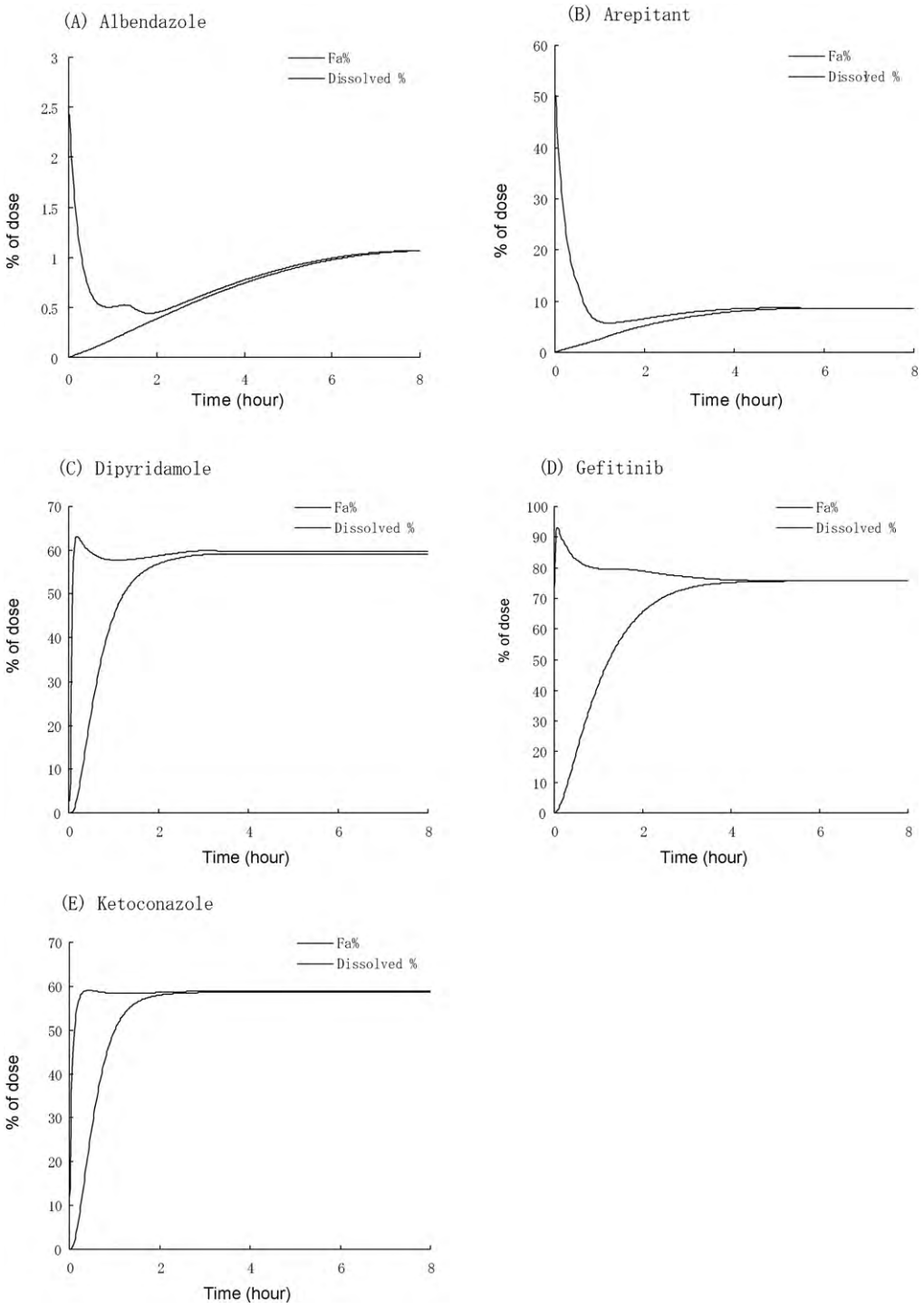

Fig. 2. Simulated *Fa%* and dissolved% vs time profile. (A) Albendazole, (B) aprepitant (5 μm), (C) dipyridamol, (D) gefinitib and (E) ketoconazole. For albendazole, the particle drifting effect was taken into account.

3.1. Albendazole

Clinically observed *Fa%* in humans with the normal stomach pH at 1400 mg dose was calculated to be 3.8% from the AUC ratio of tablet and solution formulations (*Fa%* = 100% was assumed for the latter case) (Schipper et al., 2000; Rigter et al., 2004). *Fa%* in humans with the high stomach pH was calculated to be 2.7% from the AUC ratio with and without a H2 blocker treatment (Schipper et al., 2000).

The dose number (*Do*, $Do = \text{Dose}/(V_{GI} \times S_{dissolv})$) in the stomach is 20 and the calculated concentration in the stomach was maintained at the saturated solubility for about 2 h (Fig. 3A). The simulated *Fa%* values for the normal and high stomach pH cases were 1.1% for both cases. Considering the possible experimental variation at this low solubility and low *Fa%*, these *Fa%* values would rather be in good agreement with the clinical observations. Without considering PDE, *Fa%* was predicted to be 0.5% for the normal stomach case.

Even though albendazole is a low solubility basic compound, the effect of stomach pH on *Fa%* at 1400 mg (20 mg/kg) was relatively small compared to the other model drugs. Since the dose number in the stomach is 40, enough solubilization capacity is not anticipated for this high dose case (max. 35 mg of 1400 mg (2.5%)

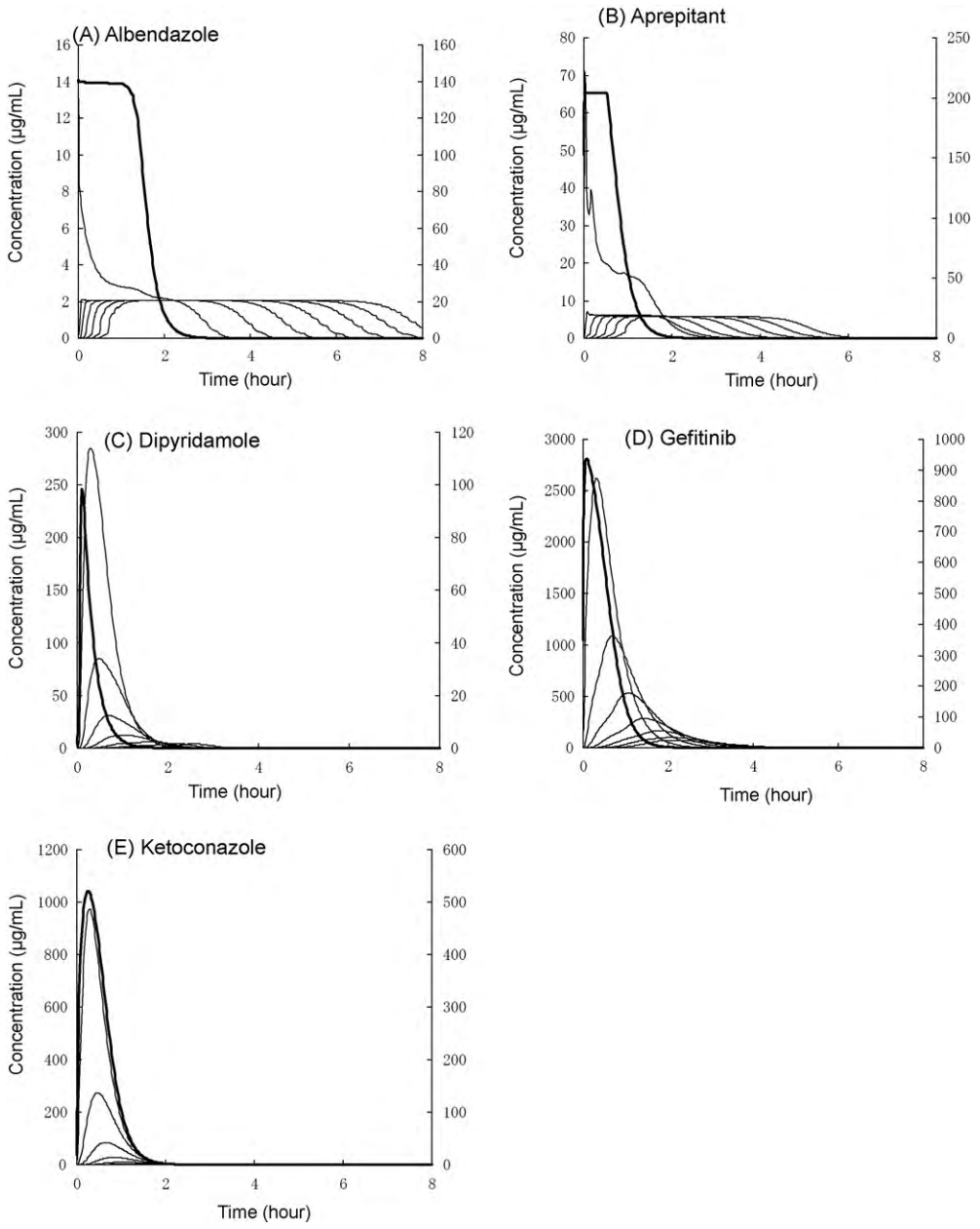

Fig. 3. Simulated dissolved drug concentration in each GI position. The bold line: the stomach (scale in the right *Y* axis), the solid lines: the small intestine (scale in the left *Y* axis) (from left to right, compartments 1–7, proximal to distal). (A) Albendazole (5 μm), (B) aprepitant, (C) dipyridamole, (D) gefitinib and (E) ketoconazole. For albendazole, the particle drifting effect was taken into account.

would be dissolved). Most of the particles reach the small intestine as incompletely dissolved (Fig. 4A). It is interesting that, at 5 mg/kg in rabbits, the AUC with the high pH stomach (pH > 5) was reported to be threefold lower than that with normal low pH stomach (pH 1) (Kohri et al., 1998). At 5 mg/kg dose with pH 1 for normal stomach pH, ca. twofold difference was simulated (other parameters were same as those for humans).

3.2. Aprepitant

Clinically observed *Fa*% of nano-particles formulation (0.2 μm, 80 mg and 125 mg) in humans with the normal stomach pH was calculated to be 70% and 62%, respectively, from absolute bioavailability (67% and 59%, respectively) and total clearance (CL = 0.85 mL/min/kg, hepatic blood flow = 20 mL/min/kg) assuming that hepatic clearance is the main clearance route (aprepitant interview form). By taking the mid-value, *Fa*% for 100 mg was estimated to be 66%. Human *Fa*% of micronized particles (100 mg) was reported to be 3.5-fold smaller than that of nano-particles (Wu et al., 2004). Therefore, *Fa*% of 100 mg micronized formulation (5 μm) was calculated to be 19%.

The dose number in the stomach is 2. The estimated dissolved drug concentration in the stomach was maintained at the saturated solubility for 1 h (Fig. 3B). In the case of micronized formulation, the particles larger than 3 μm were estimated to reach the small intestine as incompletely dissolved (Fig. 4B). The simulated *Fa*% values for the micronized (5 μm) and nano-particle (0.2 μm) API cases were 9% and 28%, respectively. Without PDE, simulated *Fa*% was 7% for nano-particles, suggesting that the consideration of PDE decreased the discrepancy between the simulation and clinical observation for nano-particle formulation. This was in good agreement with the previous simulation results for oral absorption of

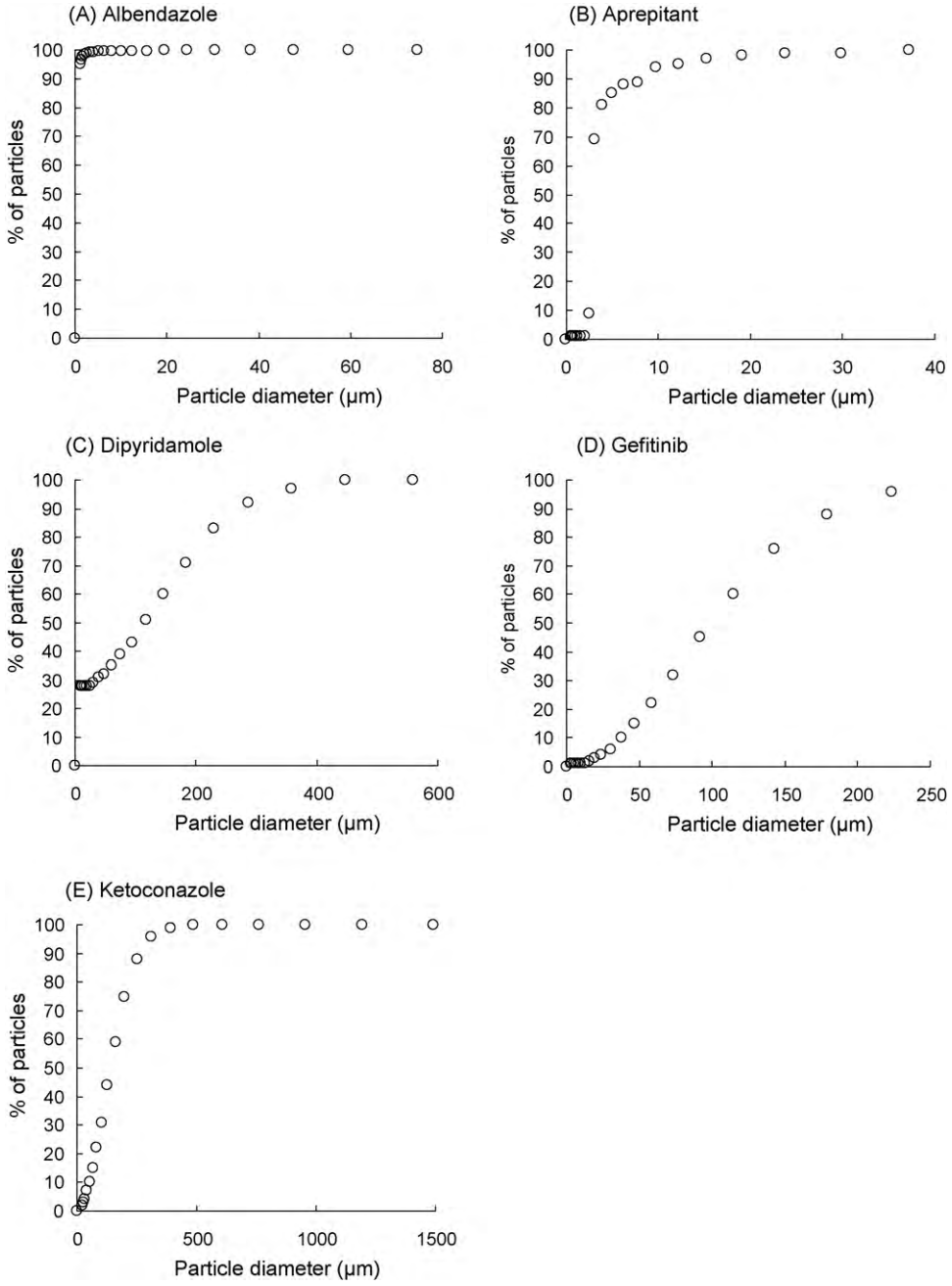

Fig. 4. Percentage of the particles incompletely dissolved during the stomach transition and reached the small intestine. (A) Albendazole (5 μm), (B) aprepitant, (C) dipyridamole, (D) gefinitib and (E) ketoconazole. For albendazole, the particle drifting effect was taken into account.

nano-particle formulation of danazol and cilostazol in dogs, further supporting that PDE can explain the increase of *Fa%* by nano-particle formulation (Sugano, 2010).

3.3. Dipyridamole

Clinically observed *Fa%* in humans with normal stomach pH (57% at 50 mg dose) was calculated from the absolute bioavailability (52%) and total clearance (2 mL/min/kg) assuming that hepatic clearance is the main clearance route (Bjornsson and Mahony, 1983; Russell et al., 1994). *Fa%* in humans with high pH stomach (36% at 50 mg dose) was calculated from the AUC ratio of 0.63 with and without H2 blocker treatment (Russell et al., 1994).

The particle size (75 μm) was back calculated from the dissolution profile of the commercial tablet at pH 4.5 (Fig. 1A) (Zhou et al., 2005). This particle size also appropriately simulated the dissolution at pH 6.5 (Fig. 1A), as well as in FaSSIF (data not shown) (Takano et al., 2006). However, when using this particle size, the dissolution rate at pH 1.2 was over-estimated more than 10-fold. Since the dissolution of API particles is very rapid at pH 1.2, the disintegration of the tablet could be the rate-limiting step at this pH. Therefore, the release of API particles from the tablet was taken into account (the bold line in Fig. 1A. 15%, 35%, 48% and 86% release at 2, 3, 4, 5 min, respectively). The solid surface pH in the stomach was estimated to be pH 2.9 (Mooney–Stella equation) and pH 3.1 (experimental value) (Vertzoni et al., 2007), which are significantly higher than that of the stomach pH of 1.8.

The dose number in the stomach is <0.007 and the estimated dissolved drug concentration in the stomach did not reach the saturated solubility (Fig. 3C). Even though $Do < 1$, the particles larger

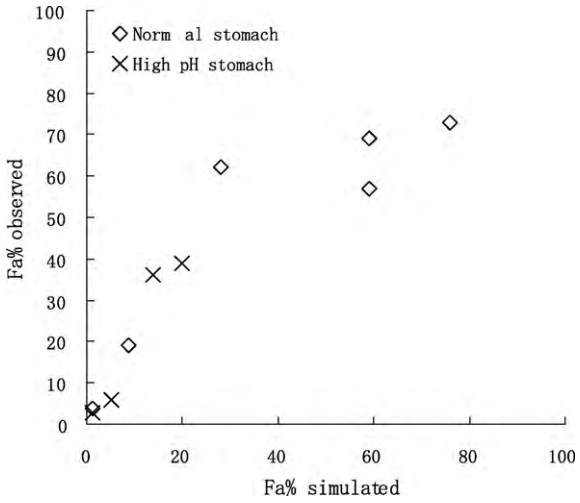

Fig. 5. Simulated and observed *Fa%*. For albendazole and aprepitant nano-particle formulation, PDE was taken into account.

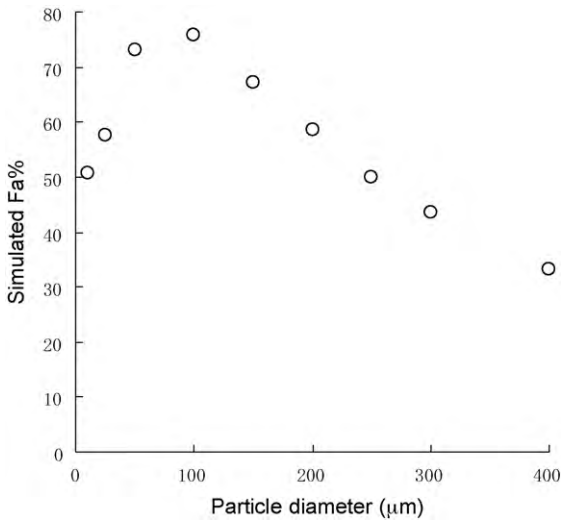

Fig. 6. *Fa%* vs particle diameter. Ketoconazole was used as a model drug.

than 30 μm were estimated to reach the small intestine as >30% incompletely dissolved (Fig. 4C). Simulated *Fa%* values for the normal and high stomach pH cases were 59% and 14%, respectively. These values are in good agreement with the clinical observations.

3.4. Gefitinib

Clinically observed *Fa%* in fasted state humans with normal stomach pH was calculated as the relative bioavailability against the AUC in the fed state assuming that oral absorption was complete in the fed state (*Fa%* in the fed state was calculated to be 100% from the bioavailability (78%) and the hepatic clearance (500 mL/min)) (Gefitinib interview form). The fed/fasted AUC ratio was reported to be 1.37 (Gefitinib interview form). Therefore, *Fa%* in the fasted state with the normal stomach was calculated to be 73%. In addition, the AUC ratio in the high/normal stomach pH was 0.53 (Bergman et al., 2007). Therefore, *Fa%* with the high pH stomach (fasted) was calculated to be 39%. The particle size (30 μm) was back calculated from the initial dissolution profile of the commercial tablet in FaSSIF (data not shown) (Takano et al., 2006). The solid surface pH was estimated to be pH 3.2 (Mooney–Stella equation) and pH 5.0 (Serajuddin method in the human gastric fluid) (Wilson et al., 2009).

The dose number in the stomach is <0.2 and the estimated dissolved drug concentration in the stomach did not reach the saturated solubility (Fig. 3D). Even though $Do < 1$, the particles larger than 70 μm were estimated to reach the small intestine as >30% incompletely dissolved (Fig. 4D). *Fa%* values for the normal and high stomach pH cases were 76% and 20%, respectively. These values are in good agreement with the clinical observations.

3.5. Ketoconazole

Clinically observed *Fa%* in humans was calculated as the relative bioavailability of the tablet formulation against the pre-dissolved formulation (69% with the normal stomach and 5.8% with the high pH stomach) (Lelawongs et al., 1988). Since the AUC of the pre-dissolved formulation in the fasted state is almost the same with that in the fed state, it would be appropriate to assume that this formulation showed almost complete absorption. The particle size (200 μm) was back calculated from the dissolution profile of the commercial tablet at pH 4.5 (Fig. 1B) (Zhou et al., 2005). This particle size also appropriately simulated the dissolution at pH 1.2 and 6.5 (Fig. 1B), as well as in FaSSIF (data not shown) (Takano et al., 2006). The solid surface pH was estimated to be pH 2.9 (Mooney–Stella equation) (Mooney et al., 1981) and pH 3.2 (Serajuddin method in the human gastric fluid) (Vertzoni et al., 2007).

The dose number in the stomach is <0.03 and the estimated dissolved drug concentration in the stomach did not reach the saturated solubility (Fig. 3E). Even though $Do < 1$, the particles larger than 100 μm were estimated to reach the small intestine as >30% incompletely dissolved (Fig. 4E). *Fa%* values for the normal and high stomach pH cases were 59% and 5%, respectively. These values are in good agreement with the clinical observations.

The particle sizes of dipyridamole, gefitinib and ketoconazole estimated from the dissolution test were relatively large even though they are low solubility compounds. Since both dissolution in the stomach and concentration reduction in the small intestine become faster as the particle size of a drug was reduced, it was theoretically suggested that there is an optimal particle size to effectively utilize the low stomach pH to dissolve a weak base drug to enhance oral absorption of the drug. Fig. 5 shows the predicted particle size dependency of *Fa%* for ketoconazole. The relatively large particle sizes of dipyridamole, ketoconazole and gefitinib might be appropriate from the view of oral absorption of a weak basic drug in humans with normal stomach pH. In contrast, the particle size of albendazole and aprepitant are smaller than those of the other model drugs. The dose number of albendazole and aprepitant in the stomach are greater than 1 and the concentration in the stomach was simulated to reach the saturated solubility (Fig. 3A and B), suggesting that sufficient dissolution in the stomach cannot be expected. Actually, the negative effect of H2 blocker on the oral absorption of albendazole is much less than those for dipyridamole, gefitinib and ketoconazole (Table 3). In this case, smaller particle size might be beneficial for these drugs as is for undissociable drugs (Fig. 6).

The prediction strategy is important considering the real drug discovery situation. Usually, the particle size data of API and dissolution test data of API and a formulation are available. With these data, we can first check the predictability of the mNB equation (Sugano et al., 2007). If this prediction failed, we should take the disintegration process into account or apply the correction factor in the mNB equation. In addition, an validation with a preclinical animal study would be important to further ensure the reliability of the mode, especially for P_{eff} assessment.

In a certain commercial software (current version), precipitation was assumed to occur as first order kinetics. The first order kinetic constant and the particle size of the precipitated drug are arbitrar-

ily given by the user to fit to the observed data (Sutton, 2009) (or the default value of 900 s^{-1} is used). In addition, the difference of free base and salt cannot be treated by the theoretical framework of the commercial software, since the solid surface pH, solubility product of salts, and nucleation process are not taken into account. The GUT framework has advantages over a commercial software as it is oriented to a fully mechanistic molecular based approach.

In conclusion, *Fa*% of free weak base drugs was simulated using the mNB equation to represent both dissolution and particle growth of a drug in the GI tract. It should be stressed that this approach is only valid for a free base, but not for its salts (and solution formulations). For the latter cases, a nucleation model equation is critical to appropriate simulate the precipitation rate of free form in the intestine (Sugano, 2009d). In addition, when the API changes its solid form such as transforming to a hydrate, further modifications of the model equations would be required.

Acknowledgements

The author would like to thank Dr. Takashi Mano and Ms. Kelly Jones for their thorough reading of this manuscript.

References

Adson, A., Ruab, T.J., Burton, P.S., Barsuhn, C.L., Hilgers, A.R., Audus, K.L., Ho, N.F.H., 1994. Quantitative approaches to delineate paracellular diffusion in cultured epithelial cell monolayers. J. Pharm. Sci. 83, 1529–1530.

Avdeef, A., 2003. Absorption and Drug Development. Wiley-Interscience, NJ, Hoboken.

Avdeef, A., 2010. Leakiness and size exclusion of paracellular channels in cultured epithelial cell monolayers—interlaboratory comparison. Pharm. Res. 27, 480–489.

Avdeef, A., Artursson, P., Neuhoff, S., Lazorova, L., Grasjo, J., Tavelin, S., 2005. Caco-2 permeability of weakly basic drugs predicted with the double-sink PAMPA pK_a (flux) method. Eur. J. Pharm. Sci. 24, 333–349.

Avdeef, A., Tsinman, K., Tsinman, O., Sun, N., Voloboy, D., 2009. Miniaturization of powder dissolution measurement and estimation of particle size. Chem. Biodiversity 6, 1796–1811.

Bergman, E., Forsell, P., Persson, E.M., Knutson, L., Dickinson, P., Smith, R., Swaisland, H., Farmer, M.R., Cantarini, M.V., Lennernaes, H., 2007. Pharmacokinetics of gefitinib in humans: the influence of gastrointestinal factors. Int. J. Pharm. 341, 134–142.

Bjornsson, T.D., Mahony, C., 1983. Clinical pharmacokinetics of dipyridamole. Thromb. Res., 93–104.

Cao, X., Leyva, N., Anderson, S.R., Hancock, B.C., 2008. Use of prediction methods to estimate true density of active pharmaceutical ingredients. Int. J. Pharm. 355, 231–237.

Clarysse, S., Psachoulias, D., Brouwers, J., Tack, J., Annaert, P., Duchateau, G., Reppas, C., Augustijns, P., 2009. Postprandial changes in solubilizing capacity of human intestinal fluids for BCS Class II drugs. Pharm. Res. 26, 1456–1466.

Diaz, D., Bernad, J.B., Mora, J.G., Llanos, C.M.E., 1998. Complexation and solubility behavior of albendazole with some cyclodextrins. Pharm. Dev. Technol. 3, 395–403.

Dressman, J.B., Amidon, G.L., Reppas, C., Shah, V.P., 1998. Dissolution testing as a prognostic tool for oral drug absorption: immediate release dosage forms. Pharm. Res. 15, 11–22.

Escher, B., Berger, C., Bramaz, N., Kwon, J.H., Richter, M., Tsinman, O., Avdeef, A., 2008. Membrane–water partitioning, membrane permeability and baseline toxicity. Environ. Toxicol. Chem. 27, 909–918.

Galia, E., Nicolaides, E., Horter, D., Lobenberg, R., Reppas, C., Dressman, J.B., 1998. Evaluation of various dissolution media for predicting in vivo performance of class I and II drugs. Pharm. Res. 15, 698–705.

Glomme, A., März, J., Dressman, J., 2006. Predicting the intestinal solubility of poorly soluble drugs. In: Testa, B., Krämer, S., Wunderli-Allenspach, H., Folkers, G. (Eds.), Pharmacokinetic Profiling in Drug Research. Wiley-VCH, Zurich, pp. 259–280.

Hintz, R.J., Johnson, K.C., 1989. The effect of particle size distribution on dissolution rate and oral absorption. Int. J. Pharm. 51, 9–17.

Jinno, J.-i., Kamada, N., Miyake, M., Yamada, K., Mukai, T., Odomi, M., Toguchi, H., Liversidge, G.G., Higaki, K., Kimura, T., 2006. Effect of particle size reduction on dissolution and oral absorption of a poorly water-soluble drug, cilostazol, in beagle dogs. J. Control. Release 111, 56–64.

Johnson, K.C., 2003. Dissolution and absorption modeling: model expansion to simulate the effects of precipitation, water absorption, longitudinally changing intestinal permeability, and controlled release on drug absorption. Drug Dev. Ind. Pharm. 29, 833–842.

Kohri, N., Yamayoshi, Y., Iseki, K., Sato, N., Todo, S., Miyazaki, K., 1998. Effect of gastric pH on the bioavailability of albendazole in rabbits. Pharm. Pharmacol. Commun. 4, 267–270.

Kortejaervi, H., Urtti, A., Yliperttula, M., 2007. Pharmacokinetic simulation of biowaiver criteria: the effects of gastric emptying, dissolution, absorption and elimination rates. Eur. J. Pharm. Sci. 30, 155–166.

Lelawongs, P., Barone, J.A., Colaizzi, J.L., Hsuan, A.T.M., Mechlinski, W., Legendre, R., Guarnieri, J., 1988. Effect of food and gastric acidity on absorption of orally administered ketoconazole. Clin. Pharm. 7, 228–235.

Lennernäs, H., 2007. Modeling gastrointestinal drug absorption requires more in vivo biopharmaceutical data: experience from in vivo dissolution and permeability studies in humans. Curr. Drug Metab. 8, 645–657.

Li, C.-Y., Zimmerman, C.L., Wiedmann, T.S., 1996. Diffusivity of bile salt/phospholipid aggregates in mucin. Pharm. Res. 13, 535–541.

Mooney, K.G., Mintun, M.A., Himmelstein, K.J., Stella, V.J., 1981. Dissolution kinetics of carboxylic acids. I: effect of pH under unbuffered conditions. J. Pharm. Sci. 70, 13–22.

Morihara, M., Aoyagi, N., Kaniwa, N., Kojima, S., Ogata, H., 2001. Assessment of gastric acidity of Japanese subjects over the last 15 years. Biol. Pharm. Bull. 24, 313–315.

Okazaki, A., Mano, T., Sugano, K., 2008. Theoretical dissolution model of polydisperse drug particles in biorelevant media. J. Pharm. Sci. 97, 1843–1852.

Oliver, R.E., Jones, A.F., Rowland, M., 1998. What surface of the intestinal epithelium is effectively available to permeating drugs? J. Pharm. Sci. 87, 634–639.

Parrott, N., Lukacova, V., Fraczkiewicz, G., Bolger, M.B., 2009. Predicting pharmacokinetics of drugs using physiologically based modeling—application to food effects. AAPS J. 11, 45–53.

Pudipeddi, M., Zannou, E.A., Vasanthavada, M., Dontabhaktuni, A., Royce, A.E., Joshi, Y.M., Serajuddin, A.T.M., 2008. Measurement of surface pH of pharmaceutical solids: a critical evaluation of indicator dye-sorption method and its comparison with slurry pH method. J. Pharm. Sci. 97, 1831–1842.

Rigter, I.M., Schipper, H.G., Koopmans, R.P., Van Kan, H.J.M., Frijlink, H.W., Kager, P.A., Guchelaar, H.J., 2004. Relative bioavailability of three newly developed albendazole formulations: a randomized crossover study with healthy volunteers. Antimicrob. Agents Chemother. 48, 1051–1054.

Russell, T.L., Berardi, R.R., Barnett, J.L., O'Sullivan, T.L., Wagner, J.G., Dressman, J.B., 1994. pH-related changes in the absorption of dipyridamole in the elderly. Pharm. Res. 11, 136–143.

Sawamoto, T., Haruta, S., Kurosaki, Y., Higaki, K., Kimura, T., 1997. Prediction of the plasma concentration profiles of orally administered drugs in rats on the basis of gastrointestinal transit kinetics and absorbability. J. Pharm. Pharmacol. 49, 450–457.

Schipper, H.G., Koopmans, R.P., Nagy, J., Butter, J.J., Kager, P.A., Van Boxtel, C.J., 2000. Effect of dose increase or cimetidine co-administration on albendazole bioavailability. Am. J. Trop. Med. Hyg. 63, 270–273.

Serajuddin, A.T.M., 2007. Salt formation to improve drug solubility. Adv. Drug Deliv. Rev. 59, 603–616.

Sugano, K., 2008. Theoretical comparison of hydrodynamic diffusion layer models used for dissolution simulation in drug discovery and development. Int. J. Pharm. 363, 73–77.

Sugano, K., 2009a. Estimation of effective intestinal membrane permeability considering bile micelle solubilisation. Int. J. Pharm. 368, 116–122.

Sugano, K., 2009b. Introduction to computational oral absorption simulation. Expert Opin. Drug Metab. Toxicol. 5, 259–293.

Sugano, K., 2009c. Oral absorption simulation for poor solubility compounds. Chem. Biodiversity 6, 2014–2029.

Sugano, K., 2009d. A simulation of oral absorption using classical nucleation theory. Int. J. Pharm. 378, 142–145.

Sugano, K., 2009e. Theoretical investigation of passive intestinal membrane permeability using Monte Carlo method to generate drug-like molecule population. Int. J. Pharm. 373, 55–61.

Sugano, K., 2009f. Theoretical investigation of passive intestinal membrane permeability using Monte Carlo method to generate drug like molecule population. Int. J. Pharm. 373, 55–61.

Sugano, K., 2010. Possible reduction of effective thickness of intestinal unstirred water layer by particle drifting effect. Int. J. Pharm. 387, 103–109.

Sugano, K., Kataoka, M., Mathews, C., Yamashita, d.C.S., 2010. Prediction of food effect by bile micelles on oral drug absorption considering free fraction in intestinal fluid. Eur. J. Pharm. Sci. 40, 118–124.

Sugano, K., Nabuchi, Y., Machida, M., Aso, Y., 2003. Prediction of human intestinal permeability using artificial membrane permeability. Int. J. Pharm. 257, 245–251.

Sugano, K., Okazaki, A., Sugimoto, S., Tavornvipas, S., Omura, A., Mano, T., 2007. Solubility and dissolution profile assessment in drug discovery. Drug Metab. Pharmacokinet. 22, 225–254.

Sugano, K., Takata, N., Machida, M., Saitoh, K., Terada, K., 2002. Prediction of passive intestinal absorption using bio-mimetic artificial membrane permeation assay and the paracellular pathway model. Int. J. Pharm. 241, 241–251.

Sutton, S.C., 2009. Role of physiological intestinal water in oral absorption. AAPS J. 11, 277–285.

Takano, R., Furumoto, K., Shiraki, K., Takata, N., Hayashi, Y., Aso, Y., Yamashita, S., 2008. Rate-limiting steps of oral absorption for poorly water-soluble drugs in dogs; prediction from a miniscale dissolution test and a physiologically-based computer simulation. Pharm. Res. 25, 2334–2344.

Takano, R., Sugano, K., Higashida, A., Hayashi, Y., Machida, M., Aso, Y., Yamashita, S., 2006. Oral absorption of poorly water-soluble drugs: computer simulation of fraction absorbed in humans from a miniscale dissolution test. Pharm. Res. 23, 1144–1156.

van de Waterbeemd, H., Gifford, E., 2003. ADMET in silico modelling: towards prediction paradise? Nat. Rev. Drug Discov. 2, 192–204.

Vertzoni, M., Pastelli, E., Psachoulias, D., Kalantzi, L., Reppas, C., 2007. Estimation of intragastric solubility of drugs. Pharm. Res. 24, 909–917.
Vogt, M., Kunath, K., Dressman, J.B., 2008. Dissolution improvement of four poorly water soluble drugs by cogrinding with commonly used excipients. Eur. J. Pharm. Biopharm. 68, 330–337.
Wilson, C.G., O'Mahony, B., Connolly, S.M., Cantarini, M.V., Farmer, M.R., Dickinson, P.A., Smith, R.P., Swaisland, H.C., 2009. Do gastrointestinal transit parameters influence the pharmacokinetics of gefitinib? Int. J. Pharm. 376, 7–12.
Wu, Y., Loper, A., Landis, E., Hettrick, L., Novak, L., Lynn, K., Chen, C., Thompson, K., Higgins, R., Batra, U., Shelukar, S., Kwei, G., Storey, D., 2004. The role of biopharmaceutics in the development of a clinical nanoparticle formulation of MK-0869: a Beagle dog model predicts improved bioavailability and diminished food effect on absorption in human. Int. J. Pharm. 285, 135–146.
Yu, L.X., Amidon, G.L., 1999. A compartmental absorption and transit model for estimating oral drug absorption. Int. J. Pharm. 186, 119–125.
Zhou, R., Moench, P., Heran, C., Lu, X., Mathias, N., Faria, T.N., Wall, D.A., Hussain, M.A., Smith, R.L., Sun, D., 2005. pH-dependent dissolution in vitro and absorption in vivo of weakly basic drugs: development of a canine model. Pharm. Res. 22, 188–192.